


Article

# Amplified Detection of the Aptamer–Vanillin Complex with the Use of Bsm DNA Polymerase

Mariia Andrianova \*, Natalia Komarova, Vitaliy Grudtsov, Evgeniy Kuznetsov and Alexander Kuznetsov 

Scientific-Manufacturing Complex Technological Centre, 1–7 Shokin Square, Zelenograd, 124498 Moscow, Russia; nat.v.kom@gmail.com (N.K.); vitaliyatgrudcov@gmail.com (V.G.); kev@tcen.ru (E.K.); kae@tcen.ru (A.K.)

\* Correspondence: smariika1987@gmail.com; Tel.: +7-(499)-734-45-21

Received: 30 November 2017; Accepted: 20 December 2017; Published: 26 December 2017

**Abstract:** The electrochemical detection of interactions between aptamers and low-molecular-weight targets often lacks sensitivity. Signal amplification improves the detection of the aptamer-analyte complex; Bsm DNA polymerase was used to amplify the signal from the interaction of vanillin and its aptamer named Van\_74 on an ion-sensitive field-effect transistor (ISFET)-based biosensor. The aptamer was immobilized on the ISFET sensitive surface. A short DNA probe was hybridized with the aptamer and dissociated from it upon vanillin addition. A free probe interacted with a special DNA molecular beacon initiated the Bsm DNA polymerase reaction that was detected by ISFET. A buffer solution suitable for both aptamer action and Bsm DNA polymerase activity was determined. The ISFET was shown to detect the Bsm DNA polymerase reaction under the selected conditions. Vanillin at different concentrations ( $1 \times 10^{-6}$ – $1 \times 10^{-8}$  M) was detected using the biosensor with signal amplification. The developed detection system allowed for the determination of vanillin, starting at a  $10^{-8}$  M concentration. Application of the Bsm DNA polymerase resulted in a 15.5 times lower LoD when compared to the biosensor without signal amplification (10.1007/s00604-017-2586-4).

**Keywords:** aptasensor; aptamer; signal amplification; Bsm DNA polymerase; ISFET; vanillin

## 1. Introduction

Aptamers are typically, single-stranded oligonucleotide (DNA or RNA) molecules <100-bp that can bind to other molecules with high specificity and affinity. Aptamers have been generated against a wide variety of targets including small molecules such as metal ions [1], aminoglycoside antibiotics [2], cocaine [3], adenosine [4] and theophylline [5]. The selective binding abilities of aptamers were employed to develop different sensors [6,7]. A variety of aptamer-based sensors for low-molecular-weight substrates have been developed recently including electrochemical [8–11] and optical [12–14].

Electrochemical aptasensors are one of the main types of sensors based on aptamers, especially for low-weight targets. The main feature of electrochemical sensors is the use of different labels and enhancements to amplify the signal since the signal from the interaction of the target with the aptamer is rather weak. Different modifications of aptamers and labels are used to amplify biosensing events. The main amplification approaches use nanoparticles [15], quantum dots [16,17], DNAzymes [18], a ferrocene redox probe [9], modification with methylene blue [19,20], and fluorescent ligands [21].

The field effect transistor (FET)-based sensor is a type of electrochemical sensor, which can be considered as an integrated device containing a receptor layer (aptamer) that selectively recognizes and binds the target compound and a signal transducer, and represented by an ion-selective field effect transistor (ISFET) that registers the recognition [22]. ISFET sensors exhibit significant advantages over other signal transducers including low manufacturing costs have been described in the literature. The label-free and reagentless aptamer-based sensor for adenosine allows for the detection of  $5 \times 10^{-5}$  M

of adenosine [23]. The detection scheme was based on the dehybridization of a DNA probe upon the addition of adenosine to an aptamer-complement probe system. Furthermore, a sensor for cocaine with Au nanoparticles as the amplifying labels was developed [24]. The limit for the detection of cocaine was  $1 \times 10^{-6}$  M. Additionally, there is an aptamer-modified silicon nanowire field-effect transistor for  $K^+$  [25], and a biosensor for adenosine triphosphate based on a hairpin DNA aptamer coupled with a field-effect transistor has been described in [26].

In this work, a new chemical amplification approach for the detection of aptamer-vanillin interaction on the ISFET with the use of Bsm DNA polymerase reaction is presented. The key moment of amplification is in the enzymatic reaction, which is initiated after the hybridized probe leaves the transistor surface with the aptamer upon the reaction of the aptamer and the target. The principle of Bsm DNA polymerase reaction was taken from [27] and adapted for measurements with the selected aptamer for vanillin. The aptamer for the low-molecular-weight target (vanillin) was previously obtained by us using a Capture-SELEX technique [28]. To conclude, an electrochemical biosensor with amplification consisting of the signal transducer (ISFET), recognition layer (aptamer for vanillin), and reaction solution (Bsm DNA polymerase reaction mixture) was developed during this work. This allowed us to decrease the limit of detection of vanillin by 15.5 times in comparison with the biosensor without amplification [28].

## 2. Materials and Methods

### 2.1. Materials

Bsm DNA polymerase, large fragment, Bsm buffer, dNTP solution, TBE electrophoresis buffer, and SYBR Gold dye were all purchased from Thermo Fisher Scientific (Waltham, MA, USA). Vanillin and 3-aminopropyltriethoxysilane were from Sigma Aldrich (St. Louis, MO, USA). Azidobutyric NHS ester and Cu(II)-TBTA reagent were obtained from Lumiprobe (Moscow, Russia). Streptavidin-coated magnetic beads were supplied by New England Biolabs (Ipswich, MA, USA). All ssDNA sequences (Supplementary Material, Table S1) were synthesized by DNA Synthesis Ltd. (Moscow, Russia). The following buffers were used:

Selection buffer: 20 mM Tris-HCl (pH 7.6), 100 mM NaCl, 5 mM KCl, 2 mM  $MgCl_2$ , 1 mM  $CaCl_2$ .

Low molarity selection buffer: 2 mM Tris-HCl (pH 7.3), 5 mM NaCl, 1 mM KCl, 1 mM  $MgCl_2$ , 0.5 mM  $CaCl_2$ .

Bsm buffer: 20 mM Tris-HCl (pH 8.8), 10 mM KCl, 10 mM  $(NH_4)_2SO_4$ , 2 mM  $MgSO_4$ , 0.1% (v/v) Tween 20.

Wash/Binding Buffer: 0.5 M NaCl, 20 mM Tris-HCl (pH 7.5), 1 mM ethylenediaminetetraacetic acid.

### 2.2. ISFET Fabrication

An n-type ISFET was fabricated using standard 1.2  $\mu m$  FD SOI CMOS technology at the SMC Technological Centre, Zelenograd, Russia [29]. The gate dielectric consisted of 10 nm  $SiO_2$  covered by 100 nm  $Ta_2O_5$ , (thermal oxidation of PVD tantalum film at 850 °C in  $O_2$ , 10 min). The transistor channel size was  $100 \times 6 \mu m$ .

### 2.3. Fluorescence Measurement of Bsm DNA Polymerase Reaction

The amount of Cy3-labelled DNA was monitored by Cy3 fluorescence. Measurements were carried out on a Tecan Infinite M200 microplate spectrofluorimeter (Tecan, Zurich, Switzerland) using excitation at 540 nm and emission at 570 nm.

### 2.4. Aptamer Selection

The aptamer for vanillin was selected from the ssDNA library according to the Capture-SELEX procedure [2] in the SMC Technological Centre. Two mM of vanillin was used as the target for selection. B1\_biotin was used as the capture probe and B1\_bank as the initial ssDNA library. The B1\_bank

consisted of two primer binding sites of 18 and 19 nt, and a random fragment of 50 nt, which was separated by capture-sequencing of 12 nt (complementary to B1\_biotin) to 10 and 40 nt. The selected aptamer for vanillin has the sequence 5'-CGACCAGCTCATTCTCAGGAGAAACATGGAGTCTCGATGATAGTAGGAGCGGCGGAACGTAGGAAGAGAGGATGACGGAGGATCCGAGCTCACAGTC-3'. The name of the aptamer is Van\_74, according to the sequencing of selected aptamers (among 83 sequences) [28].

### 2.5. Aptamer Immobilization

Immobilization of the aptamer on the gate surface was conducted via “click-chemistry” in three stages [22]: (1) 3% aminopropyltriethoxysilane in methanol for 30 min, (2) 4.4–6.0 mM azidobutyric NHS ester in 0.1 M Tris/HCl, pH 8.65 for 4 h, (3)  $5 \times 10^{-7}$  M alkyne-modified aptamer with 0.05 mM copper-containing reagent (Cu(II)-TBTA) and 2 mM ascorbic acid in the same buffer overnight. After aptamer immobilization, the aptamer was hybridized with short complementary probes for 2 h.

### 2.6. ISFET Measurements

The operating subthreshold mode of the ISFET was determined from the  $I$ - $V_G$  curves ( $V_{DS} = 0.1$  V); the threshold voltage  $V_t$  and subthreshold slope  $S$  were used. Time-dependent changes in the current  $I_{DS}$  ( $V_G = \text{const}$ ) were measured and the surface potential change  $\Delta\phi_i \approx \frac{S}{S_0} n\phi t \frac{I_{i+1} - I_i}{I_i}$  was used as a signal. All measurements were carried out in a well-like structure made of organic ink deposited onto the surface of the crystal with a pneumatic dispenser Nordson EFD Ultimius V pneumatic dispenser (Westlake, OH, USA; 5.7 bar at 22 °C) and Janome JR2303 robot positioning system (Tokyo, Japan) [30]. Time-dependent changes of  $I_{DS}$  ( $V_G = \text{const}$ ) were recorded in a well-like structure containing 25–30  $\mu\text{L}$  of buffer and during the record 1–1.5  $\mu\text{L}$  of target was added.

### 2.7. Aptamer Characterization by PAGE [28]

Washed streptavidin-coated magnetic beads were incubated with the capture probe B1\_biotin (100  $\mu\text{L}$  of beads ( $c = 4$  mg/mL): 50  $\mu\text{L}$  of Wash/Binding Buffer with 400 pmol of B1\_biotin) for 2 h. After incubation, the beads were well washed in the Selection buffer and incubated with the aptamer (50  $\mu\text{L}$  of the Selection buffer with 800 pmol of aptamer) overnight with interval mixing (1200 rpm for 30 s, 9 min 30 s without mixing) using an Eppendorf Thermomixer Comfort (Hamburg, Germany). The unbound ssDNA was washed away by rinsing the particles with the SB seven times. Weakly bound sequences were removed by incubating the particles at 28 °C for 15 min, followed by seven washes with SB.

Modified magnetic beads were added to the buffer containing vanillin, and incubated for 1 h at 21 °C with constant mixing at 850 rpm (5  $\mu\text{L}$  of beads for each sample of the total volume of 50  $\mu\text{L}$  of beads). Aliquots of 5  $\mu\text{L}$  from the washout were used in PCR (20  $\mu\text{L}$  of PCR premix for each sample) and the eluted aptamer was amplified. The reaction mixture contained 1.0  $\mu\text{M}$  of primers, 0.2 mM  $\text{MgCl}_2$ , 0.25 mM of each dNTP, and 0.06 U/ $\mu\text{L}$  Taq DNA polymerase in 75 mM Tris-HCl (pH 8.8 at 25 °C), 20 mM  $(\text{NH}_4)_2\text{SO}_4$ , and 0.01% ( $v/v$ ) Tween 20. Amplification was carried out in a Tercyk Thermocycler (Moscow, Russia) and included an initial denaturation step at 95 °C for 5 min; 12 cycles of 95 °C for 30 s, 66 °C for 30 s, and 72 °C for 30 s; and a final extension step at 72 °C for 2 min.

Five  $\mu\text{L}$  of the PCR product without purification were loaded to the nondenaturing PAGE. After 1 h of separation at 120 V in a Mini Protein Tetra Cell System (Bio-Rad, Hercules, CA, USA), the gel was stained with SYBR Gold and scanned by a Bio-1000F scanner (Microtek, Hsinchu, Taiwan). The GelQuant.NET software (Biochemlabsolutions.com, University of California, San Francisco, CA, USA) was used to analyze the intensity of DNA strips in the gel.

## 3. Results

The scheme assumed that the immobilized aptamer on the ISFET surface was hybridized with the DNA probe, which was released from the aptamer during the addition of vanillin (Figure 1).

This dehybridized DNA probe then participated in the Bsm DNA polymerase reaction which was detected by the ISFET. The main components of this reaction were a hairpin fluorescence probe (FP), a short primer (PR), and a dehybridized DNA probe (DP), which can hybridize with FP and open the hairpin. After that, the hairpin annealed with the primer and triggered the polymerization reaction [27]. Polymerase has a strong strand displacement activity and lacks exonuclease activities, so the DP was displaced and hybridized to another FP. Therefore, this was the amplification of the signal at a low concentration of DP. Amplification was monitored in situ with the use of a highly sensitive ISFET (Figure 1).

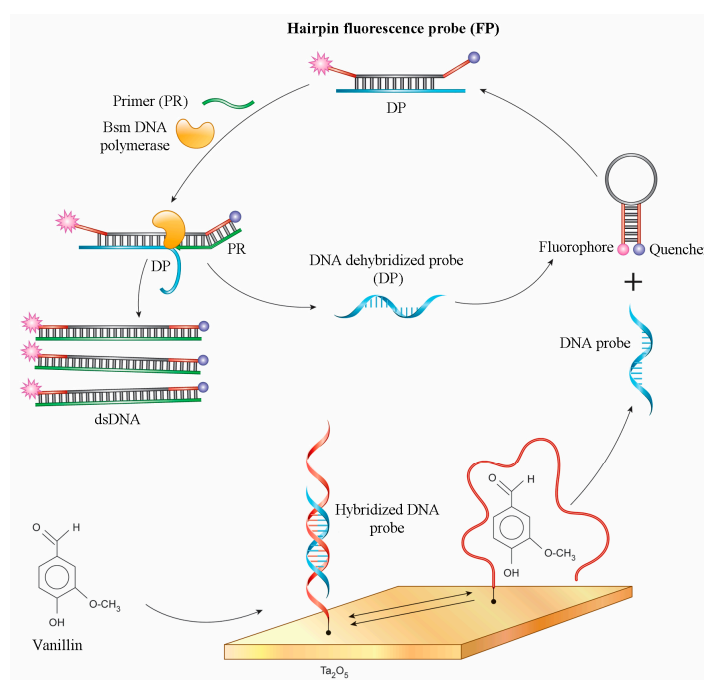


**Figure 1.** Detection scheme: release of the dehybridized DNA probe during aptamer-vanillin complex formation and the Bsm DNA polymerase reaction with probe detected by ISFET.

### 3.1. Optimization of Operating Conditions

The idea of amplifying the signal from a small amount of ssDNA with the use of Bsm DNA polymerase was taken from [27]. However, FP, DP and PR were designed corresponding to the aptamer sequence (Table 1).

**Table 1.** Oligonucleotide sequences used in Bsm DNA polymerase reaction. The underlined sequence is a capture sequence.

Sequence Name	Sequence, 5'-3' Direction	Comment
Van_74	CGACCAGTCATTCTCCTCAGGAGAAACATGGAG <u>TCTCGATGATAGTAGGAGCGGCGGA</u> ACGTAGGAAGAGAGGATGACCGAGGATCCGA GTCACCAGTC	Aptamer for vanillin
B1	CATCGAGACTCC	Capture probe without biotin
DP	ACCACATCGAGACTCCTGTGCCTTT	Bsm dehybridization probe
FP	FAM-TCTTGGFCFCAGGAGTCTCGATGTGGTATT GTGTCCAAGA-BHQ1	Fluorescence probe
PR	TCTTGGAC	Primer

The aptamer, Van\_74, was developed using the capture-SELEX protocol [2], which implied a capture-sequence in its structure that was used for ssDNA library fixation onto the solid support via hybridization with the capture-probe B1\_biotin. So, part of the designed DP contained sequence of

the capture-probe B1\_biotin, which was complementary to the capture-sequence of Van\_74, to ensure its dehybridization upon the addition of vanillin. The other nucleotides in the DP sequence were optimized to non-complement the Van\_74 sequence and partly complement the FP to break down its hairpin. Moreover, the DP and FP were designed to ensure the single possible stem-loop structure for the FP predicted by the Mfold web server [31] with free energy of  $-13.35$  kJ at  $21$  °C [32] (Figure S1). The nucleotide sequence for the stem was analogous to the probe used in [27], and the loop part was complementary to the DP sequence. The primer sequence was the same as in the original paper [27].

Initially, the conditions under which detection will take place were optimized before the fabrication of the sensor. It is known that an aptamer can form an effective complex with a target only under specific conditions (buffer composition, salt concentration, pH, temperature), which mostly correspond to the conditions of the aptamer selection process [33–36]. The aptamer for vanillin presented in this work was selected in the Selection buffer with a total molarity of  $128$  mM (pH 7.6) and at the temperature of  $21$  °C. However, according to supplier information, Bsm DNA polymerase is active in a wide range of temperatures from  $30$  to  $63$  °C (with an optimum activity at  $60$  °C) and should be used in Bsm buffer with a total molarity of  $42$  mM (pH 8.8) and content of surfactant (Tween 20).

It was shown that the aptamer did not bind vanillin in the Bsm buffer (Figure 2 and Figure S2). For this purpose, magnetic beads coated with the aptamer (via B1) were incubated in vanillin solutions ( $1.5$  mM) in the Bsm buffer and the Selection buffer. PCR amplification of the washout showed that the signal (band intensity) from the Bsm buffer with vanillin had no significant difference from the background (Figure 2 and Figure S2). On the other hand, incubation of the modified magnetic beads in the Selection buffer with vanillin showed the formation of the aptamer-vanillin complex (Figure 2 and Figure S2).

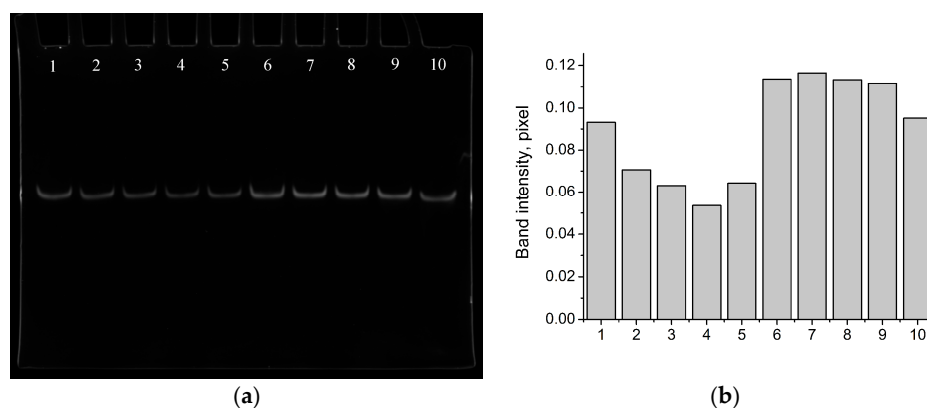


**Figure 2.** Nondenaturing PAGE (photo without any modification) of the PCR amplified (16 cycles) washout probes from the magnetic beads modified with B1/Van\_74 (a) and image analysis of phoresis with GelQuant.NET (b) for different incubation buffers: (1) Selection buffer with vanillin ( $1.5$  mM); (2) Selection buffer with vanillin ( $1.5$  mM), repeat; (3) Selection buffer; (4) Selection buffer, repeat; (5) Selection buffer, repeat; (6) Bsm buffer with vanillin ( $1.5$  mM); (7) Bsm buffer with vanillin ( $1.5$  mM), repeat; (8) Bsm buffer; (9) Bsm buffer, repeat; and (10) Bsm buffer, repeat.

Thus, the choice of working buffer was essential for several reasons. It had an impact on aptamer behavior, the Bsm DNA polymerase reaction, and the ISFET sensitivity. The sensitivity of ISFET greatly depends on the distance of charges from the interface, the so-called Debye length, beyond which potential change cannot be properly detected [37]. The Debye length is a function of electrolyte concentration [38]. Thus, the choice of a buffer with low molarity was preferable. Previously, it has been shown that aptamers can bind vanillin not only in the Selection buffer, but in the low molarity selection buffer [28]. Thus, the investigation of the Bsm DNA polymerase reaction in the low molarity selection buffer was undertaken (Figure 3).

As seen in Figure 3, the maximum Bsm DNA polymerase activity corresponded to the Selection buffer and DP and the minimum to low molarity Selection buffer and B1. In general, the polymerase activity was greatest when using DP as a probe compared to B1. This behavior was obviously due to the length of the probe and the interaction with FP. Since the DP was longer than B1 by 14 bp and was complementary to FP at least by 6 bp more, it was more likely to open the hairpin of the FT, which prevents the polymerase reaction. Therefore, we decided to use a DP probe in the low molarity buffer on the ISFET for the Bsm DNA polymerase reaction.

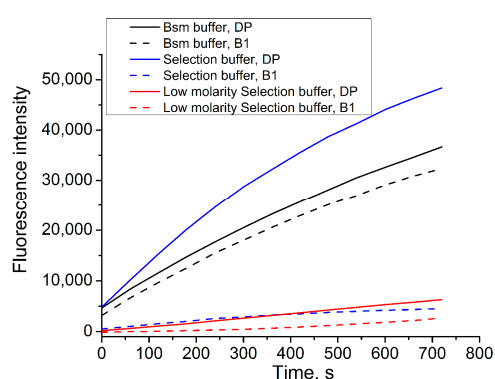


**Figure 3.** Kinetics of Bsm DNA polymerase reaction (after subtraction of the background) monitored by spectrofluorimeter in different buffers and probes. Conditions: buffer, 0.2 mM dNTP, 0.05 pmol/ $\mu$ L FP, 1.6 pmol/ $\mu$ L PR, 0.1 U/ $\mu$ L BSM DNA polymerase, 0.1 pmol/ $\mu$ L DP/B1.

For this, the DP probe was tested as a dehybridization probe from aptamer Van\_74 during the addition of vanillin. For this purpose, nondenaturing PAGE of washouts from the modified magnetic beads was carried out (Figure 4 and Figure S3). The obtained results showed that the B1 probe could be changed by DP in the experiments with the aptamer and target: the complementary between DP and Van\_74 could be broken during the vanillin addition.

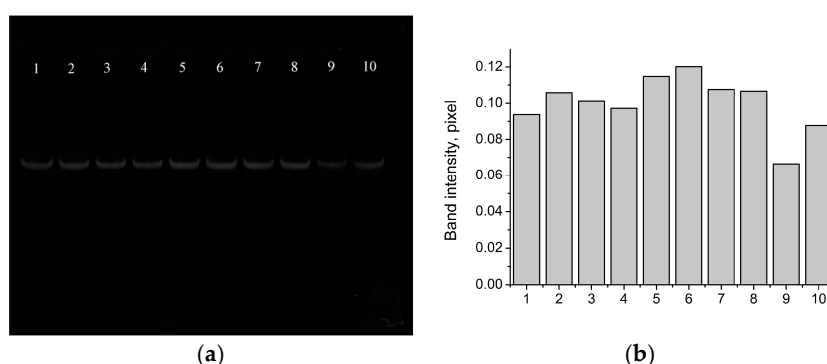


**Figure 4.** Nondenaturing PAGE (photo without any modification) of PCR amplified (10 cycles) washout probes from magnetic beads modified with DP/Van\_74 (a) and image analysis of phoresis with GelQuant.NET (b) for different vanillin concentrations in low molarity Selection buffer: (1)  $1 \times 10^{-3}$  M; (2)  $1 \times 10^{-3}$  M, repeat; (3)  $2.5 \times 10^{-4}$  M; (4)  $2.5 \times 10^{-4}$  M, repeat; (5)  $6.25 \times 10^{-5}$  M; (6)  $6.25 \times 10^{-5}$  M, repeat; (7)  $1.6 \times 10^{-5}$  M; (8)  $1.6 \times 10^{-5}$  M, repeat; (9) low molarity selection buffer; and (10) low molarity selection buffer, repeat.

To sum up, the obtained results presented in this section are:

- Aptamer for vanillin could not perform in the Bsm buffer and could bind vanillin in the Selection buffer and low molarity selection buffer.



- Bsm DNA polymerase is active in a low molarity selection buffer and the greatest activity is with DP compared to B1.
- B1 probe can be replaced by DP as a dehybridization probe from the aptamer Van\_74 during the vanillin addition.

### 3.2. Bsm DNA Polymerase Reaction on the ISFET

The response of the ISFET to the Bsm DNA polymerase reaction in the homogenous solution was tested. A well-like structure made of organic ink on the ISFET surface was filled with reaction solution (low molarity selection buffer, 0.2 mM dNTP, 0.05 pmol/ $\mu$ L FP, 1.6 pmol/ $\mu$ L PR, 0.1 U/ $\mu$ L BSM DNA polymerase) except the DP. Then, different concentrations of DP were added to the well while the drain current ( $I_{DS}$ ) induced by the reaction was measured, and then, according to the  $I_{DS}$  surface potential change, was calculated. The decrease in surface potential after the addition of the DP was proportional to its concentration (Figure 5a). The main criteria for the reaction proceeding was the slope (mV/s) after DP addition (Figure 5b). Thus, the limit of detection (LoD) of DP on the ISFET in low molarity selection buffer was  $4.0 \times 10^{-9}$  M.

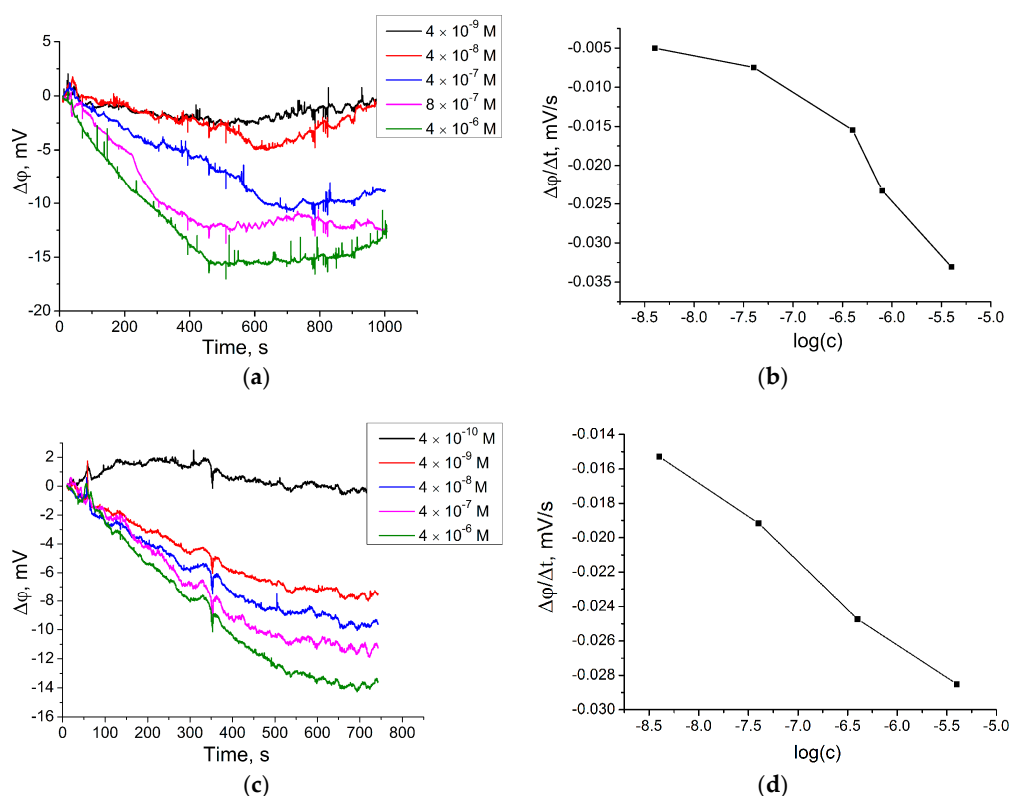


**Figure 5.** (a) Real time signal of the ISFET (in  $\Delta\phi$ , with background subtraction) during the Bsm DNA polymerase reaction in homogenous solution in low molarity selection buffer initiated (30–40 s) by the addition of DP at different concentrations (final concentration is marked on the picture); (b) Slope ( $\Delta\phi/\Delta t$ ) dependence on DP concentration calculated from real time signal curves. Reaction conditions: 0.2 mM dNTP, 0.05 pmol/ $\mu$ L FP, 1.6 pmol/ $\mu$ L PR, 0.1 U/ $\mu$ L BSM DNA polymerase; (c) Real time signal of the ISFET (in  $\Delta\phi$ , with background subtraction) during the Bsm DNA polymerase reaction in homogenous solution in low molarity selection buffer initiated (30–40 s) by the addition of DP at different concentrations (final concentration is marked on the picture); (d) Slope ( $\Delta\phi/\Delta t$ ) dependence on DP concentration calculated from real time signal curves. Reaction conditions: 0.2 mM dNTP, 1.0 pmol/ $\mu$ L FP, 1.6 pmol/ $\mu$ L PR, 0.1 U/ $\mu$ L BSM DNA polymerase.

The same reaction, but with a higher concentration of FP (1 pmol/ $\mu$ L) is given on Figure 5c,d. The quantity of FP is important for the amplification reaction as the Bsm DNA polymerase can act until all single stranded FP become double stranded DNA. Thus, the quantity of FP should be greater than DP so the amplification of the signal from DP can be seen (FP  $\gg$  DP). Therefore, it was shown that an increase in FP concentration led to the enhancement of the signal from low concentrations of DP. The LoD of DP on the ISFET in these conditions was  $4.0 \times 10^{-9}$  M. The Bsm DNA polymerase reaction on the ISFET in Bsm buffer and Selection buffer is presented in the Supplementary Material (Figures S4 and S5). It was shown that in the BSM buffer, the reaction proceeded faster than in the low molarity selection buffer and could be detected by the ISFET. The polymerase reaction in the Selection buffer was not detected by the ISFET at the applied concentration of DP. Furthermore, the Bsm DNA polymerase reaction on the ISFET modified with Van\_74/probe DP in the low molarity selection buffer was held. This experiment was supposed to show the response of the modified ISFET, where the sensitive surface carried negative charge due to DNA, to the Bsm DNA polymerase. It turned out that the direction of the surface potential change remained the same as for nonmodified ISFET surface (Figure S6).

### 3.3. Amplified Detection of the Aptamer–Vanillin Complex with the Bsm DNA Polymerase and ISFET

The aptamer for vanillin was immobilized on the ISFETs surface and hybridized with DP. Aliquots with different concentrations of vanillin were added to a well-like structure onto the ISFETs surface containing the Bsm DNA polymerase reaction mixture. For the measurements, two reaction mixtures were used; the difference between them was in the concentration of FP. The concentration of FP in Mixture 1 was 0.05 pmol/ $\mu$ L, and Mixture 2 was 1 pmol/ $\mu$ L, 20 times higher (Figure 6). The addition of vanillin to the system in concentrations from  $1 \times 10^{-6}$  to  $1 \times 10^{-8}$  M caused an equally significant decrease in the surface potential change. The signal from the addition of vanillin in a concentration of  $1 \times 10^{-9}$  M did not significantly differ from the background. Additionally, the signal from only the dehybridization of DP during the vanillin addition in the reaction condition did not differ from the background (Figure 6b), which testifies in favor of the amplification technique.

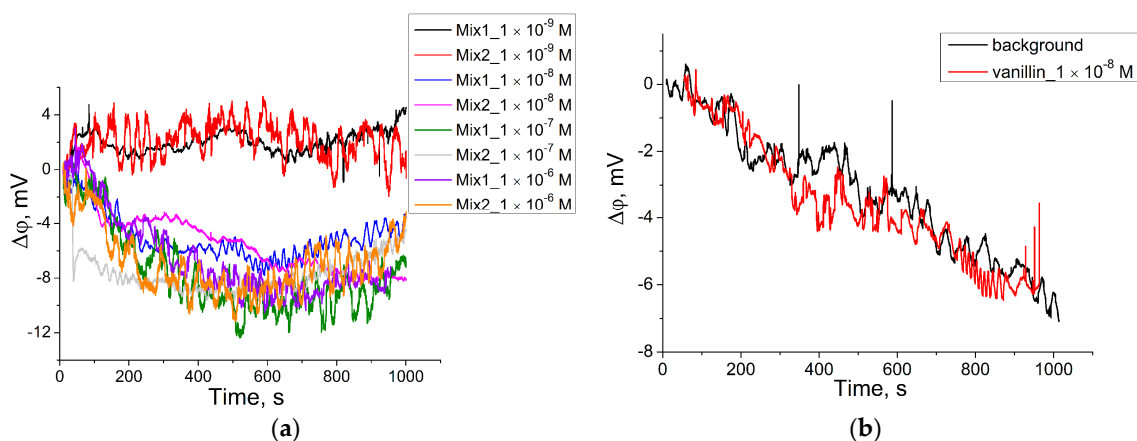


**Figure 6.** (a) Dependence of response (with background subtraction) of modified with Van\_74/DP ISFETs to the Bsm DNA polymerase reaction with the addition of different vanillin concentrations. Conditions: **mix1**—low molarity selection buffer, 0.2 mM dNTP, FP 0.05 pmol/ $\mu$ L, PR 1.6 pmol/ $\mu$ L, Bsm DNA polymerase 0.1 U/ $\mu$ L; **mix2**—low molarity selection buffer, 0.2 mM dNTP, FP 1.0 pmol/ $\mu$ L, PR 1.6 pmol/ $\mu$ L, Bsm DNA polymerase 0.1 U/ $\mu$ L, T = 22 °C; (b) Real time signal of the ISFET (in  $\Delta\phi$ ) of modified with Van\_74/DP ISFETs to the addition of vanillin (final concentration  $1 \times 10^{-8}$ ) concentration. Conditions: low molarity selection buffer, 0.2 mM dNTP, PR 1.6 pmol/ $\mu$ L, Bsm DNA polymerase 0.1 U/ $\mu$ L.



The proposed approach allowed us to conduct a qualitative analysis of vanillin (not less than  $1 \times 10^{-8}$  M). Compared with our previous research [29], the limit of detection of vanillin during this research was increased by 15.5 times (Table 2). The possibility to carry out only qualitative analysis and not quantitative can be explained by the time required for reaction proceeding: diffusion of vanillin to the ISFET surface, the interaction between the aptamer and vanillin, and the dehybridization of DP, initiation of the Bsm reaction, etc. The reaction time in the experiments was limited due to evaporation in the open well-like system. The use of a microfluidic system may solve this problem in future.

The fabricated biosensor had good reproducibility and stability. The relative standard deviation (RSD) of the biosensor response to  $10^{-8}$  M of vanillin was approximately 7% for five successive measurements. In the practical performance of the sensor, approximately 500 s of exposure time was required for each measurement.

The main mechanism of ISFET sensitivity is determined by the surface potential change at the interface of surface/solution. This surface potential change comes from a change in the electrochemical potential of electrons in the solution during the enzymatic reaction and change in the quantity of DNA probes adsorbed on the ISFET surface. The electrochemical potential of the solution is the summary of the electrochemical potentials of all components in the system: buffer reagents, salts, enzyme, and substrates. During the enzymatic reaction, the total electrochemical potential of the solution changes due to local pH change and this change causes a change in the surface potential, which is detected by the ISFET. At low concentrations of vanillin (and, by extension, low concentration of desorbed DP) the ISFET is more sensitive to the reaction when compared to probe dehybridization (desorption from the surface), which is the difference in the values of electrochemical potential connected to each process. Local pH change is due to the release of proton ( $H^+$ ) during the polymerase reaction: the phosphodiester bond is formed between the  $\alpha$ -phosphate of the incoming dNTP and 3'-OH group of deoxyribose, the chemical reaction generates a pyrophosphate and proton molecule [39].

#### 4. Discussion

The rapid development of microelectronic technologies in the last few decades has led to the fact that CMOS technology has now become a reliable and inexpensive technological platform for creating electrochemical sensors. This has led to the appearance of miniature biosensors on silicon chips. In contrast to conventional biosensors, CMOS biosensors have a low cost, are portable, can easily integrate into more complex systems, and have low energy consumption. In combination with aptamers, CMOS biosensors can serve as a promising universal platform for creating diagnostic systems. However, one of the drawbacks for wide use of such a platform is the low detection limits of low-weight molecules (see Table 2). One of the potential solutions to increase the detection limit is to use chemical amplification of the signal.

In comparison with other FET sensors presented in Table 2, the obtained sensor showed equal or better performance in the determination of the small molecule, particularly in, vanillin. It should be noted that the limit of detection of the protein molecules was lower in comparison to low-weight molecules because more charge was introduced into the system that resulted in a larger disturbance of electromagnetic field near the sensitive surface.

Despite the promising results demonstrated in this study, the use of the Bsm DNA polymerase reaction as the amplification technique has some limitations. In this research, only a qualitative analysis of vanillin was shown. This drawback can be overcome by the use of a microfluidic system. One more limitation is to select a working buffer where both the aptamer and the enzyme can work. Despite these limitations, the use of the Bsm DNA polymerase reaction with the combination of ISFET and aptamer showed successful results in the amplification of the signal from the interaction of aptamer Van\_74 and small molecule vanillin.

**Table 2.** Sensors based on FETs and aptamers presented in the literature.

Substance	LoD, M	Type	Reference
Low-weight molecules			
Adenosine	$5 \times 10^{-5}$	Si-ISFET	[23]
Adenosine	$1 \times 10^{-11}$	Graphene-FET	[40]
Cocaine	$1 \times 10^{-6}$	Si-ISFET	[24]
K <sup>+</sup>	$K_{\text{ass}} = (2.18 \pm 0.44) \times 10^6$	Si-ISFET	[25]
Bisphenol A	$1 \times 10^{-12}$ – $1 \times 10^{-14}$	Carbon-FET	[41]
ATP	-	FET	[26]
Vanillin (our previous work)	$1.55 \times 10^{-7}$	Si-ISFET	[28]
Vanillin	$1 \times 10^{-8}$	Si-ISFET	This work
Protein molecules			
Thrombin	$2.5 \times 10^{-8}$	Si-ISFET	[42]
Thrombin	$7 \times 10^{-7}$	Si-ISFET	[43]
Thrombin	$5 \times 10^{-8}$	Polypyrrole-FET	[44]
Thrombin	$2 \times 10^{-11}$	Carbon-FET	[45]
Vascular endothelial growth factor	$1.04 \times 10^{-9}$ – $1.04 \times 10^{-10}$	Si-ISFET	[46]
IgE	$K_{\text{diss}} = 4.7 \times 10^{-8}$	Graphene-ISFET	[47]
IgE	$2.5 \times 10^{-10}$	Carbon-FET	[48]
Interferon gamma	$8.3 \times 10^{-11}$	Graphene-ISFET	[49]
Platelet-derived growth factor	$5 \times 10^{-12}$	Carbon-FET	[50]
Platelet-derived growth factor	-	Diamond-FET	[51]

## 5. Conclusions

The ISFET-based biosensor to detect the interaction between the aptamer and small target—vanillin—using the Bsm DNA polymerase reaction as a chemical amplification was developed. It allowed us to carry out qualitative analysis of vanillin and improve the LoD of vanillin by 15.5 times when compared to a biosensor without amplification.

Further improvements of the biosensor are planned by fabricating a microfluidic system on the surface of the chip. This avoids the evaporation of reagents and minimizes the signal-to-noise ratio.

**Supplementary Materials:** The following are available online at <http://www.mdpi.com/1424-8220/18/1/49/s1>, Table S1: Oligonucleotide sequences used in the work, Figure S1: Stem-loop structure for the FP predicted by Mfold web, Figure S2: Nondenaturing PAGE (photo without any modification) of PCR amplified (14 cycles) washout probes from magnetic beads modified with B1/Van\_74, Figure S3: Nondenaturing PAGE (photo without any modification) of PCR amplified (14 cycles) washout probes from magnetic beads modified with DP/Van\_74, Figure S4: Real time signal of the ISFET (in  $\Delta\phi$ ) during Bsm DNA polymerase reaction in homogenous solution in Bsm buffer initiated (30–40 s) by addition of DP at different concentration (final concentration are marked on the picture), Figure S5: Real time signal of the ISFET (in  $\Delta\phi$ ), Figure S6: Real time signal of the modified with Van\_74 ISFET (in  $\Delta\phi$ , with background subtraction).

**Acknowledgments:** This work was supported by the Russian Science Foundation (project #16-19-10697).

**Author Contributions:** M.A. designed and performed the experiments on the ISFET, designed and performed the experiments of the aptamer by nondenaturing PAGE, did measurements of Bsm DNA polymerase on the spectrofluorometer, analyzed the data and wrote the paper. N.K. obtained the aptamer for vanillin, suggested the idea of using the Bsm DNA polymerase as the amplification approach and designed the components (oligonucleotides) of this reaction. V.G. carried out measurements of modified ISFETs and checked the language of the article. E.K. was responsible for the development of ISFETs. A.K. coordinated the work and did the provision of scientific activities in general. All authors discussed and reviewed the manuscript. We thank the Center of Collective Use “Functional Control and Diagnostics of Micro- and Nanosystem Engineering based on R&D Technological Center” (Moscow, Zelenograd) for allowing access to their equipment.

**Conflicts of Interest:** The authors declare no conflict of interest.

## References

- Rajendran, M.; Ellington, A.D. Selection of fluorescent aptamer beacons that light up in the presence of zinc. *Anal. Bioanal. Chem.* **2008**, *390*, 1067–1075. [CrossRef] [PubMed]
- Stoltenburg, R.; Nikolaus, N.; Strehlitz, B. Capture-SELEX: Selection of DNA Aptamers for Aminoglycoside Antibiotics. *J. Anal. Methods Chem.* **2012**, *2012*. [CrossRef] [PubMed]

3. Stojanovic, M.N.; de Prada, P.; Landry, D.W. Aptamer-Based Folding Fluorescent Sensor for Cocaine. *J. Am. Chem. Soc.* **2001**, *123*, 4928–4931. [[CrossRef](#)] [[PubMed](#)]
4. Huizenga, D.E.; Szostak, J.W. A DNA Aptamer That Binds Adenosine and ATP. *Biochemistry* **1995**, *34*, 656–665. [[CrossRef](#)] [[PubMed](#)]
5. Zimmermann, G.R.; Jenison, R.D.; Wick, C.L.; Simorre, J.-P.; Pardi, A. Interlocking structural motifs mediate molecular discrimination by a theophylline-binding RNA. *Nat. Struct. Biol.* **1997**, *4*, 644–649. [[CrossRef](#)] [[PubMed](#)]
6. Tombelli, S.; Minunni, M.; Mascini, M. Analytical applications of aptamers. *Biosens. Bioelectron.* **2005**, *20*, 2424–2434. [[CrossRef](#)] [[PubMed](#)]
7. Ilgu, M.; Nilsen-Hamilton, M. Aptamers in analytics. *Analyst* **2016**, *141*, 1551–1568. [[CrossRef](#)] [[PubMed](#)]
8. Swensen, J.S.; Xiao, Y.; Ferguson, B.S.; Lubin, A.A.; Lai, R.Y.; Heeger, A.J.; Plaxco, K.W.; Soh, H.T. Continuous, Real-Time Monitoring of Cocaine in Undiluted Blood Serum via a Microfluidic, Electrochemical Aptamer-Based Sensor. *J. Am. Chem. Soc.* **2009**, *131*, 4262–4266. [[CrossRef](#)] [[PubMed](#)]
9. Ferapontova, E.E.; Olsen, E.M.; Gothelf, K.V. An RNA Aptamer-Based Electrochemical Biosensor for Detection of Theophylline in Serum. *J. Am. Chem. Soc.* **2008**, *130*, 4256–4258. [[CrossRef](#)] [[PubMed](#)]
10. Rowe, A.A.; Miller, E.A.; Plaxco, K.W. Reagentless Measurement of Aminoglycoside Antibiotics in Blood Serum via an Electrochemical, Ribonucleic Acid Aptamer-Based Biosensor. *Anal. Chem.* **2010**, *82*, 7090–7095. [[CrossRef](#)] [[PubMed](#)]
11. Wang, D.; Xiao, X.; Xu, S.; Liu, Y.; Li, Y. Electrochemical aptamer-based nanosensor fabricated on single Au nanowire electrodes for adenosine triphosphate assay. *Biosens. Bioelectron.* **2018**, *99*, 431–437. [[CrossRef](#)] [[PubMed](#)]
12. Zhou, J.; Ellis, A.V.; Kobus, H.; Voelcker, N.H. Aptamer sensor for cocaine using minor groove binder based energy transfer. *Anal. Chim. Acta* **2012**, *719*, 76–81. [[CrossRef](#)] [[PubMed](#)]
13. Feng, S.; Che, X.; Que, L.; Chen, C.; Wang, W. Rapid detection of theophylline using aptamer-based nanopore thin film sensor. In Proceedings of the 2016 IEEE SENSORS, Orlando, FL, USA, 30 October–3 November 2016; pp. 1–3.
14. Ramezani, M.; Mohammad Danesh, N.; Lavaee, P.; Abnous, K.; Mohammad Taghdisi, S. A novel colorimetric triple-helix molecular switch aptasensor for ultrasensitive detection of tetracycline. *Biosens. Bioelectron.* **2015**, *70*, 181–187. [[CrossRef](#)] [[PubMed](#)]
15. Pavlov, V.; Xiao, Y.; Shlyahovsky, B.; Willner, I. Aptamer-Functionalized Au Nanoparticles for the Amplified Optical Detection of Thrombin. *J. Am. Chem. Soc.* **2004**, *126*, 11768–11769. [[CrossRef](#)] [[PubMed](#)]
16. Hansen, J.A.; Wang, J.; Kawde, A.-N.; Xiang, Y.; Gothelf, K.V.; Collins, G. Quantum-Dot/Aptamer-Based Ultrasensitive Multi-Analyte Electrochemical Biosensor. *J. Am. Chem. Soc.* **2006**, *128*, 2228–2229. [[CrossRef](#)] [[PubMed](#)]
17. Zhang, H.; Jiang, B.; Xiang, Y.; Zhang, Y.; Chai, Y.; Yuan, R. Aptamer/quantum dot-based simultaneous electrochemical detection of multiple small molecules. *Anal. Chim. Acta* **2011**, *688*, 99–103. [[CrossRef](#)] [[PubMed](#)]
18. Sun, A.; Qi, Q.; Wang, X.; Bie, P. Porous platinum nanotubes labeled with hemin/G-quadruplex based electrochemical aptasensor for sensitive thrombin analysis via the cascade signal amplification. *Biosens. Bioelectron.* **2014**, *57*, 16–21. [[CrossRef](#)] [[PubMed](#)]
19. Xiao, Y.; Piorek, B.D.; Plaxco, K.W.; Heeger, A.J. A reagentless signal-on architecture for electronic, aptamer-based sensors via target-induced strand displacement. *J. Am. Chem. Soc.* **2005**, *127*, 17990–17991. [[CrossRef](#)] [[PubMed](#)]
20. Baker, B.R.; Lai, R.Y.; Wood, M.S.; Doctor, E.H.; Heeger, A.J.; Plaxco, K.W. An Electronic, Aptamer-Based Small-Molecule Sensor for the Rapid, Label-Free Detection of Cocaine in Adulterated Samples and Biological Fluids. *J. Am. Chem. Soc.* **2006**, *128*, 3138–3139. [[CrossRef](#)] [[PubMed](#)]
21. Xu, Z.; Morita, K.; Sato, Y.; Dai, Q.; Nishizawa, S.; Teramae, N. Label-free aptamer-based sensor using abasic site-containing DNA and a nucleobase-specific fluorescent ligand. *Chem. Commun.* **2009**, 6445. [[CrossRef](#)] [[PubMed](#)]
22. Bergveld, P. Development of an ion-sensitive solid-state device for neurophysiological measurements. *IEEE Trans. Biomed. Eng.* **1970**, *17*, 70–71. [[CrossRef](#)] [[PubMed](#)]
23. Zayats, M.; Huang, Y.; Gill, R.; Ma, C.; Willner, I. Label-free and reagentless aptamer-based sensors for small molecules. *J. Am. Chem. Soc.* **2006**, *128*, 13666–13667. [[CrossRef](#)] [[PubMed](#)]

24. Sharon, E.; Freeman, R.; Tel-Vered, R.; Willner, I. Impedimetric or Ion-Sensitive Field-Effect Transistor (ISFET) Aptasensors Based on the Self-Assembly of Au Nanoparticle-Functionalized Supramolecular Aptamer Nanostructures. *Electroanalysis* **2009**, *21*, 1291–1296. [[CrossRef](#)]
25. Anand, A.; Liu, C.-R.; Chou, A.-C.; Hsu, W.-H.; Ulaganathan, R.K.; Lin, Y.-C.; Dai, C.-A.; Tseng, F.-G.; Pan, C.-Y.; Chen, Y.-T. Detection of K<sup>+</sup> Efflux from Stimulated Cortical Neurons by an Aptamer-Modified Silicon Nanowire Field-Effect Transistor. *ACS Sens.* **2017**, *2*, 69–79. [[CrossRef](#)] [[PubMed](#)]
26. Goda, T.; Miyahara, Y. A hairpin DNA aptamer coupled with groove binders as a smart switch for a field-effect transistor biosensor. *Biosens. Bioelectron.* **2012**, *32*, 244–249. [[CrossRef](#)] [[PubMed](#)]
27. Guo, Q.; Yang, X.; Wang, K.; Tan, W.; Li, W.; Tang, H.; Li, H. Sensitive fluorescence detection of nucleic acids based on isothermal circular strand-displacement polymerization reaction. *Nucl. Acids Res.* **2009**, *37*, e20. [[CrossRef](#)] [[PubMed](#)]
28. Kuznetsov, A.E.; Komarova, N.V.; Andrianova, M.S.; Grudtsov, V.P.; Kuznetsov, E.V. Aptamer based vanillin sensor using an ion-sensitive field-effect transistor. *Microchim. Acta* **2017**. [[CrossRef](#)]
29. Kuznetsov, A.; Andrianova, M.; Komarova, N.; Grudtsov, V.; Kuznetsov, E.; Saurov, A. Detection of aroma compound by ISFET modified with aptamer. In Proceedings of the 2017 2nd International Conference on Bio-engineering for Smart Technologies (BioSMART), Paris, France, 30 August–1 September 2017; pp. 1–3.
30. Gubanova, O.; Andrianova, M.; Saveliev, M.; Komarova, N.; Kuznetsov, E.; Kuznetsov, A. Fabrication and package of ISFET biosensor for micro volume analysis with the use of direct ink writing approach. *Mater. Sci. Semicond. Process.* **2016**. [[CrossRef](#)]
31. Zuker, M. Mfold web server for nucleic acid folding and hybridization prediction. *Nucl. Acids Res.* **2003**, *31*, 3406–3415. [[CrossRef](#)] [[PubMed](#)]
32. SantaLucia, J. A unified view of polymer, dumbbell, and oligonucleotide DNA nearest-neighbor thermodynamics. *Proc. Natl. Acad. Sci. USA* **1998**, *95*, 1460–1465. [[CrossRef](#)] [[PubMed](#)]
33. Hianik, T.; Ostatná, V.; Sonlajtnerova, M.; Grman, I. Influence of ionic strength, pH and aptamer configuration for binding affinity to thrombin. *Bioelectrochemistry* **2007**, *70*, 127–133. [[CrossRef](#)] [[PubMed](#)]
34. Yang, X.; Bing, T.; Mei, H.; Fang, C.; Cao, Z.; Shangguan, D. Characterization and application of a DNA aptamer binding to l-tryptophan. *Analyst* **2011**, *136*, 577–585. [[CrossRef](#)] [[PubMed](#)]
35. Lin, P.-H.; Yen, S.-L.; Lin, M.-S.; Chang, Y.; Louis, S.R.; Higuchi, A.; Chen, W.-Y. Microcalorimetric Studies of the Thermodynamics and Binding Mechanism between L-Tyrosinamide and Aptamer. *J. Phys. Chem. B* **2008**, *112*, 6665–6673. [[CrossRef](#)] [[PubMed](#)]
36. Wu, J.; Wang, C.; Li, X.; Song, Y.; Wang, W.; Li, C.; Hu, J.; Zhu, Z.; Li, J.; Zhang, W.; et al. Identification, Characterization and Application of a G-Quadruplex Structured DNA Aptamer against Cancer Biomarker Protein Anterior Gradient Homolog 2. *PLoS ONE* **2012**, *7*, e46393. [[CrossRef](#)] [[PubMed](#)]
37. Stern, E.; Wagner, R.; Sigworth, F.J.; Breaker, R.; Fahmy, T.M.; Reed, M.A. Importance of the Debye Screening Length on Nanowire Field Effect Transistor Sensors. *Nano Lett.* **2007**, *7*, 3405–3409. [[CrossRef](#)] [[PubMed](#)]
38. Bunimovich, Y.L.; Shin, Y.S.; Yeo, W.-S.; Amori, M.; Kwong, G.; Heath, J.R. Quantitative Real-Time Measurements of DNA Hybridization with Alkylated Nonoxidized Silicon Nanowires in Electrolyte Solution. *J. Am. Chem. Soc.* **2006**, *128*, 16323–16331. [[CrossRef](#)] [[PubMed](#)]
39. Chen, C.-Y. DNA polymerases drive DNA sequencing-by-synthesis technologies: Both past and present. *Front. Microbiol.* **2014**, *5*, 1–11. [[CrossRef](#)] [[PubMed](#)]
40. Mukherjee, S.; Meshik, X.; Choi, M.; Farid, S.; Datta, D.; Lan, Y.; Poduri, S.; Sarkar, K.; Batteredene, U.; Huang, C.-E.; et al. A Graphene and Aptamer Based Liquid Gated FET-Like Electrochemical Biosensor to Detect Adenosine Triphosphate. *IEEE Trans. Nanobiosci.* **2015**, *14*, 967–972. [[CrossRef](#)] [[PubMed](#)]
41. Lee, J.; Jo, M.; Kim, T.H.; Ahn, J.-Y.; Lee, D.; Kim, S.; Hong, S. Aptamer sandwich-based carbon nanotube sensors for single-carbon-atomic-resolution detection of non-polar small molecular species. *Lab Chip* **2011**, *11*, 52–56. [[CrossRef](#)] [[PubMed](#)]
42. Sharon, E.; Liu, X.; Freeman, R.; Yehezkeili, O.; Willner, I. Label-Free Analysis of Thrombin or Hg<sup>2+</sup> Ions by Nucleic Acid-Functionalized Graphene Oxide Matrices Assembled on Field-Effect Transistors. *Electroanalysis* **2013**, *25*, 851–856. [[CrossRef](#)]
43. Andrianova, M.S.; Grudtsov, V.P.; Komarova, N.V.; Kuznetsov, E.V.; Kuznetsov, A.E. ISFET-based Aptasensor for Thrombin Detection Using Horseradish Peroxidase. *Procedia Eng.* **2017**, *174*, 1084–1092. [[CrossRef](#)]

44. Yoon, H.; Kim, J.-H.; Lee, N.; Kim, B.-G.; Jang, J. A Novel Sensor Platform Based on Aptamer-Conjugated Polypyrrole Nanotubes for Label-Free Electrochemical Protein Detection. *ChemBioChem* **2008**, *9*, 634–641. [[CrossRef](#)] [[PubMed](#)]
45. Pacios, M.; Martin-Fernandez, I.; Borrisé, X.; del Valle, M.; Bartrolí, J.; Lora-Tamayo, E.; Godignon, P.; Pérez-Murano, F.; Esplandiú, M.J. Real time protein recognition in a liquid-gated carbon nanotube field-effect transistor modified with aptamers. *Nanoscale* **2012**, *4*, 5917. [[CrossRef](#)] [[PubMed](#)]
46. Lee, H.-S.; Kim, K.S.; Kim, C.-J.; Hahn, S.K.; Jo, M.-H. Electrical detection of VEGFs for cancer diagnoses using anti-vascular endothelial growth factor aptamer-modified Si nanowire FETs. *Biosens. Bioelectron.* **2009**, *24*, 1801–1805. [[CrossRef](#)] [[PubMed](#)]
47. Ohno, Y.; Maehashi, K.; Matsumoto, K. Label-Free Biosensors Based on Aptamer-Modified Graphene Field-Effect Transistors. *J. Am. Chem. Soc.* **2010**, *132*, 18012–18013. [[CrossRef](#)] [[PubMed](#)]
48. Maehashi, K.; Katsura, T.; Kerman, K.; Takamura, Y.; Matsumoto, K.; Tamiya, E. Label-Free Protein Biosensor Based on Aptamer-Modified Carbon Nanotube Field-Effect Transistors. *Anal. Chem.* **2007**, *79*, 782–787. [[CrossRef](#)] [[PubMed](#)]
49. Farid, S.; Meshik, X.; Choi, M.; Mukherjee, S.; Lan, Y.; Parikh, D.; Poduri, S.; Batteredene, U.; Huang, C.-E.; Wang, Y.Y.; et al. Detection of Interferon gamma using graphene and aptamer based FET-like electrochemical biosensor. *Biosens. Bioelectron.* **2015**, *71*, 294–299. [[CrossRef](#)] [[PubMed](#)]
50. Jun, J.; Lee, J.S.; Shin, D.H.; Jang, J. Aptamer-Functionalized Hybrid Carbon Nanofiber FET-Type Electrode for a Highly Sensitive and Selective Platelet-Derived Growth Factor Biosensor. *ACS Appl. Mater. Interfaces* **2014**, *6*, 13859–13865. [[CrossRef](#)] [[PubMed](#)]
51. Ruslinda, A.R.; Tajima, S.; Ishii, Y.; Ishiyama, Y.; Edgington, R.; Kawarada, H. Aptamer-based biosensor for sensitive PDGF detection using diamond transistor. *Biosens. Bioelectron.* **2010**, *26*, 1599–1604. [[CrossRef](#)] [[PubMed](#)]



© 2017 by the authors. Licensee MDPI, Basel, Switzerland. This article is an open access article distributed under the terms and conditions of the Creative Commons Attribution (CC BY) license (<http://creativecommons.org/licenses/by/4.0/>).